

NOTE

The Tidal Response of Europa

William B. Moore and Gerald Schubert

Department of Earth and Space Sciences, Institute of Geophysics and Planetary Physics,
University of California, Los Angeles, California 90095-1567
E-mail: bmoore@artemis.ess.ucla.edu

Received May 8, 2000, revised June 7, 2000

The tidal response of Europa to a time-varying potential is determined by solving the quasi-static equilibrium equations for a body composed of several uniform, Maxwell viscoelastic layers. Models in which Europa's surface ice extends all the way to the silicate mantle have weak tidal responses (~1 m vertical deflection) while models in which a liquid "ocean" underlies the ice have about 30 m peak vertical deflection. The phase-lag of the tidal response is very small (<2°) in the case of an ocean, but may be large if there is no ocean and the ice has a viscosity around 10¹³ Pa s. For models with an ocean, the product of the thickness and strength of the ice determines the tidal response, making it difficult to determine the thickness of the ice by observing the tidal deflection of Europa.

© 2000 Academic Press

1. Introduction. Europa experiences semidiurnal (1.8-day) tides as it travels around Jupiter on an eccentric orbit. These tides are superimposed on the much larger static tide which has been measured gravitationally by the Galileo mission (Anderson *et al.* 1998). The static tide reflects the behavior of Europa as an entirely fluid body, due to the very long timescales (10⁹ yr) over which the mean distance from Europa to Jupiter changes. The response of Europa to the daily tide, on the other hand, reflects the viscoelastic properties of Europa's interior on a timescale of a few days. This timescale is sufficiently short so that competent solids (ice or rock) behave differently from fluids. The response of Europa to the semidiurnal tide therefore provides information on the rheological as well as density structure of Europa's interior. In particular, the sensitivity of Europa's tidal response to the presence or absence of a subsurface layer of liquid water opens an opportunity to identify a global ocean by measuring Europa's semidiurnal tides.

Since we have no direct measurement of the properties of Europa's interior, in this paper we present the tidal response of several Europa models, consistent with the static tide measurements and laboratory measurements of the rheologies of ice and rock. The next section describes the model calculations and presents the results for radial deformation and gravity perturbation. The last section discusses the implications for using satellite based measurements to infer the properties of Europa's interior.

2. Model and results. The interior of Europa is modeled as several uniform Maxwell-viscoelastic layers and is completely specified by the radii of the layers and the values of density, viscosity, and shear modulus in each layer. Liquid layers have zero shear modulus and are treated as inviscid, since the viscosities of liquid iron and liquid water are very small. A liquid core is assumed in the calculations presented here. The effect of a solid core is to reduce deformation by several percent. The parameters of the basic model are given in Table I.

The densities are constrained by the hydrostatic models which best fit the observed gravitational field of Europa (Anderson *et al.* 1998). The shear modulus of rock is taken as 10¹¹ Pa (Turcotte and Schubert 1982). The shear modulus of ice is less well known. The tidal response of floating ice shelves on Earth (Vaughan 1995) yields a value of 0.88 × 10⁹ Pa, and a series of laboratory studies indicates a low-frequency modulus near 2 × 10⁹ Pa (Cole and Durell 1995). Previous studies have used higher values, so we will present models using a shear modulus of 10⁹ or 10¹⁰ Pa.

In a European reference frame, the time-varying potential to first order in the eccentricity is given by (Kaula 1964, Poirier *et al.* 1983, Segatz *et al.* 1988)

$$\Phi = r^2 \omega^2 e \left\{ -\frac{3}{2} P_2^0(\cos \theta) \cos \omega t + \frac{1}{4} P_2^2(\cos \theta) [3 \cos \omega t \cos 2\phi + 4 \sin \omega t \sin 2\phi] \right\}, \quad (1)$$

where r is radius from the center of Europa, ω is the orbital angular frequency (2.05 × 10⁻⁵ rad s⁻¹), e is the orbital eccentricity (0.0093), θ and ϕ are the colatitude and longitude with zero longitude at the subjovian point, t is time, and P_2^0 and P_2^2 are associated Legendre polynomials.

The problem of the spheroidal deformations of a self-gravitating sphere under the influence of the external potential (1) is solved using the method of Wolf (1994) generalized to a multilayered body under periodic tidal forcing (see also Amelung and Wolf (1994)). From Wolf (1994), the Lagrangian equations of continuity, stress equilibrium, and potential are Fourier transformed in time, yielding

$$u_{i,i} = 0 \quad (2)$$

$$\tau_{ij}^{(\partial)} = 0; \quad \tau_{ij}^{(\partial)} = -\delta_{ij} p^{(\partial)} + \mu(s) [u_{i,j} + u_{j,i}] \quad (3)$$

$$g_i^{(\Delta)} = \phi_{,i}^{(\Delta)}; \quad \phi_{,ii}^{(\Delta)} = 0, \quad (4)$$

where each variable is the complex Fourier amplitude, which is a function of frequency, $s = i\omega$; u is the displacement vector; $\tau^{(\partial)}$ is the isopotential stress tensor; $p^{(\partial)}$ is the isopotential pressure; $g^{(\Delta)}$ is the local gradient of the gravitational potential $\phi^{(\Delta)}$; and the usual index conventions apply. The isopotential $^{(\partial)}$ and local $^{(\Delta)}$ Lagrangian fields are related to the more conventional material $^{(\delta)}$ fields by

$$f^{(\delta)} = f^{(\partial)} + f_{,k}^0 (u_k - d_k) \quad (5)$$

$$f^{(\delta)} = f^{(\Delta)} + f_{,k}^0 u_k, \quad (6)$$

where f is any field, f^0 is the reference (hydrostatic) value of that field, and d is the displacement of the isopotential surface originally associated with the

TABLE I
Europa Interior Model

Layer	Thickness (km)	Density (kg m^{-3})
Core	704	5150
Mantle	742	3300
Ice/ocean	119	1000

material element. Note that the use of isopotential and local fields has decoupled (4) from (2) and (3). Gravitational–mechanical coupling occurs entirely in the boundary conditions. This is similar in spirit, if not detail, to a decoupling proposed by Richards and Hager (1984).

The complex rigidity $\mu(s)$ in (3) is s times the Fourier transform of the Maxwell stress relaxation function,

$$\mu(s) = \frac{s\mu}{s + \eta/\mu}, \quad (7)$$

where the constant μ on the right side is the elastic rigidity and η is the viscosity. The ratio μ/η is the inverse Maxwell time. It is the imaginary part of $\mu(s)$ that controls dissipation.

Equations (2)–(4) are transformed into spherical harmonics of degree 2, yielding six first-order, linear differential equations in the radial coordinate (e.g., Alterman *et al.* 1959). The four equations relating the deformation and pressure fields (mechanical quantities) are decoupled from the two equations for the potential (gravitational quantities). For constant property layers, power series solutions with three regular (positive powers of radius) and three irregular (negative powers of radius) terms exist for each field. The complete solution may therefore be represented by a six-by-six matrix of power-series coefficients in each layer. The solutions are forced to satisfy continuity of deformation, potential, and stress at each internal interface. The unknown coefficients of the three regular solutions at the center of Europa are solved for via a shooting method (Press *et al.* 1992, p. 757) which propagates the solutions from the center to the surface, where three boundary conditions (zero shear stress, continuity of potential, and jump condition on the gradient of the potential) serve as constraints.

Since the quasi-static equations (2) and (3) become degenerate when μ goes to zero (Dahlen 1974), the solutions for the mechanical quantities become arbitrary in liquid layers (an ocean or a liquid core). To resolve this problem, we treat internal free surfaces like the surface, using them as intermediate shooting points for the mechanical quantities by enforcing zero shear stress and continuity of normal stress conditions. Discontinuous jumps in the mechanical quantities across the interface are introduced as new unknowns. The solutions are then propagated to the next (radially outward) liquid–solid interface, where the two free-surface conditions are again applied, reducing the unknowns back to the three which may be constrained at the surface. The propagation of the gravitational quantities is unaffected by liquid layers.

Since the solution fields are linearly related to the forcing given by (1), they will themselves be harmonic functions of ωt with a possible phase lag (given by the ratio of the imaginary and real parts of the complex Fourier amplitude) relative to the forcing potential. The calculations reproduce analytical solutions for uniform and two-layer models to better than 10^{-3} .

Figure 1 is a normalized map of Φ as given by (1) over one-half of a European orbit starting at perijove (top left) and proceeding counterclockwise. The next half-orbit is similar, with the signs reversed. Except for a scale factor and a possible phase lag, Fig. 1 also represents the radial surface displacement u_r and the perturbation to the force of gravity Δg . Table II gives the maximum values of u_r and Δg (at 100 km altitude) as well as the surface Love numbers h_2 and k_2 for various models of Europa's rheological structure. The surface Love numbers are defined by

$$h_2 = \frac{g_0 u_r}{\Phi} \quad \text{and} \quad k_2 = \frac{\Phi_{\text{tidal}}}{\Phi}, \quad (8)$$

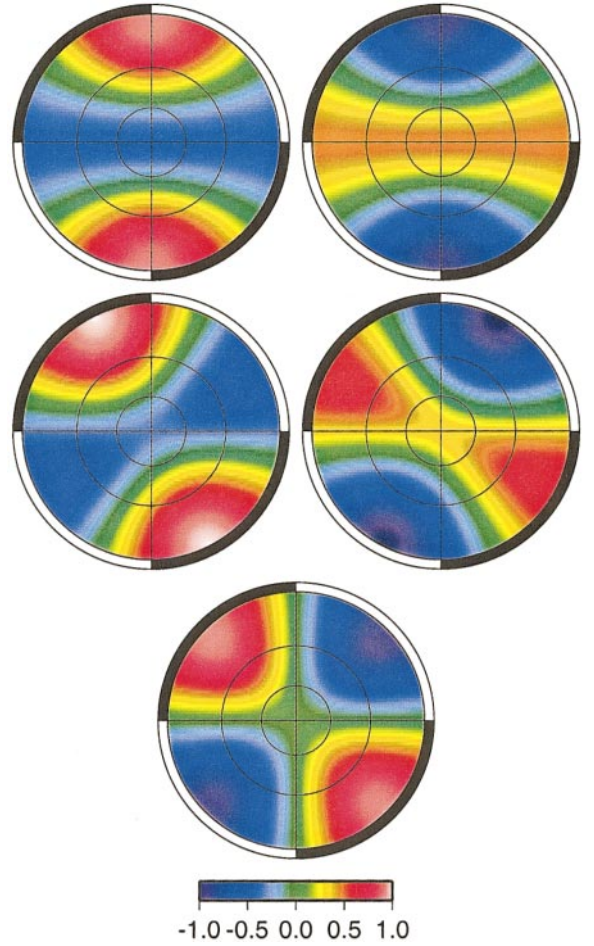


FIG. 1. Φ from (1) normalized to ± 1 plotted over the northern hemisphere of Europa beginning at perijove (top left) and proceeding counter-clockwise to apojove (top right). Lines of longitude every 90° and latitude every 30° are shown in black. Jupiter is downward. The radial displacement u_r and gravity perturbation Δg have the same contours, using the scale factors in Table II and allowing for a possible phase lag.

TABLE II
Love Numbers and Peak Radial Deflection and Gravity Perturbation at 100 km Altitude

Model	h_2	k_2	u_r (m)	Δg (mgal)
Fluid, undifferentiated	2.5	1.5	58.7	5.21
Fluid, differentiated	2.05	1.05	48.1	2.39
Elastic mantle (10^{11} Pa), no ice	1.26	0.261	29.6	-2.53
1-km ice shell (10^9 Pa)	1.26	0.261	29.6	-2.53
10-km ice shell (10^9 Pa)	1.25	0.259	29.3	-2.55
100-km ice shell (10^9 Pa)	1.16	0.241	27.2	-2.66
1-km ice shell (10^{10} Pa)	1.25	0.259	29.3	-2.55
10-km ice shell (10^{10} Pa)	1.16	0.241	27.2	-2.66
100-km ice shell (10^{10} Pa)	0.669	0.141	15.7	-3.28
No ocean (10^6 Pa)	0.770	0.163	18.1	-3.15
No ocean (10^9 Pa)	0.0271	0.0149	0.636	-4.07
No ocean (10^{10} Pa)	0.0252	0.0144	0.591	-4.08

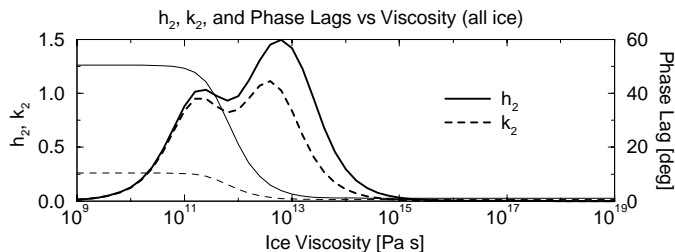


FIG. 2. h_2 , k_2 (thin lines) and their phase lags (thick lines) as a function of ice viscosity for models without a liquid ocean.

where g_0 is the acceleration of gravity at the surface and Φ_{tidal} is the potential that results from the deformation of Europa. For the fluid/elastic models in Table II there are no phase lags. Viscoelastic behavior can cause the tidal response of Europa to lag the disturbing potential.

The phase lags in the deformation (h_2) and gravity (k_2) tides for models without oceans and with an ice rigidity of 10^9 Pa and varying ice viscosity are shown in Fig. 2. These models include a thin (5 km), high-viscosity (10^{19} Pa s) ice lithosphere. Large phase lags are achieved for models with the Maxwell time (defined as viscosity divided by rigidity) of the ice layer similar to the forcing period. The double peak is due to the lithosphere. Also shown in Fig. 2 are the magnitudes of h_2 and k_2 , which show that significant tides are not raised without an ocean unless the viscosity of the ice drops below 10^{12} Pa s, an unrealistically low number for solid ice.

The phase lags are substantially altered by the presence of an ocean. The phase lag in the deformation (h_2) for a floating ice layer of varying thickness (including the 5-km lithosphere) and viscosity is shown in Fig. 3. The maximum is about 2° for the thickest shells with Maxwell times near the orbital period. The presence of a fluid layer imposes a fluid-like response on the overlying ice, strongly reducing the phase lag.

3. Implications for measurement. The difference in tidal amplitude between models with oceans and those without is apparent from Table II. More than an order of magnitude separates the two classes of models, unless the rigidity of ice approaches values around 10^6 Pa, which is three orders of magnitude below experimental values (Vaughan 1995, Cole and Durell 1995). Note, how-

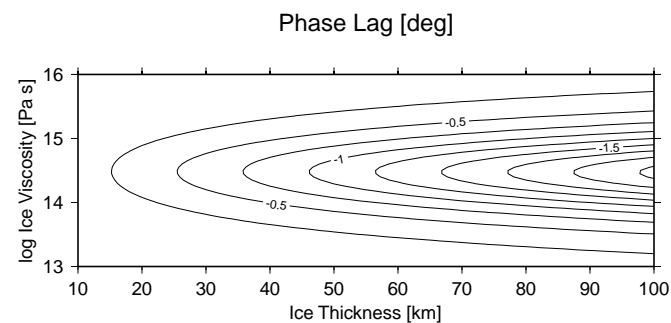


FIG. 3. Phase lag of h_2 as a function of ice viscosity and ice thickness for models with an ocean.

ever, the tradeoff between thickness and rigidity. It is clear that the product of thickness and rigidity controls the response of the decoupled shell and the two will be difficult to separate. While in principle the phase lags due to viscoelastic behavior in the ice would help to discriminate among models, these phase lags will be very small in the presence of a liquid ocean. The measurement of Δg , in addition to u_r , can help distinguish between a truly fluid response ($h_2 - k_2 = 1$) and a “mushy” viscoelastic response ($h_2 - k_2 < 1$).

In conclusion, measurements of the amplitude of the European tide to within a few meters have a reasonably good chance of identifying a subsurface ocean. Unfortunately, the thickness of the ice will be difficult to separate from the poorly known rigidity. A layer of mixed liquid and ice with a low rigidity would be distinguishable if the tidal measurements were coupled with measurements of gravity perturbations. Phase lags of the tidal response will be quite small in the presence of an ocean; large observed lags may indicate a mushy ice–liquid mixture.

ACKNOWLEDGMENTS

Stan Peale and Gregory Hoppa are sincerely thanked for their rapid and helpful reviews. This work was partially supported by NASA PG&G and NSF LExEn.

REFERENCES

- Alterman, Z., H. Jarosch, and C. L. Pekeris 1959. Oscillations of the Earth. *Proc. R. Soc. London Ser. A* **252**, 80–95.
- Amelung, F., and D. Wolf 1994. Viscoelastic perturbations of the Earth: Significance of the incremental gravitational force in models of glacial isostasy. *Geophys. J. Int.* **117**, 864–879.
- Anderson, J. D., G. Schubert, R. A. Jacobsen, E. L. Lau, and W. B. Moore 1998. Europa’s differentiated internal structure: Inferences from four Galileo encounters. *Science* **281**, 2019–2022.
- Cole, D. M., and G. D. Durell 1995. The cyclic loading of saline ice. *Philos. Mag. A* **72**, 209–229.
- Dahlen, F. A. 1974. On the static deformation of an Earth model with a fluid core. *Geophys. J. Roy. Astron. Soc.* **36**, 461–485.
- Kaula, W. M. 1964. Tidal dissipation by solid friction and the resulting orbital evolution. *Rev. Geophys.* **2**, 661–685.
- Poirier, J. P., L. Boloh, and P. Chambon 1983. Tidal dissipation in small viscoelastic ice moons: The case of Enceladus. *Icarus* **55**, 218–230.
- Press, W. H., S. A. Teukolsky, W. T. Vetterling, and B. P. Flannery 1992. *Numerical Recipes in C*. Cambridge Univ. Press, Cambridge, UK.
- Richards, M. A., and B. H. Hager 1984. Geoid anomalies in a dynamic Earth. *J. Geophys. Res.* **89**, 5987–6002.
- Segatz, M., T. Spohn, M. N. Ross, and G. Schubert 1988. Tidal dissipation, surface heat flow, and figure of viscoelastic models of Io. *Icarus* **75**, 187–206.
- Turcotte, D. L., and G. Schubert 1982. *Geodynamics*. Wiley, New York.
- Vaughan, D. G. 1995. Tidal flexure at ice shelf margins. *J. Geophys. Res.* **100**, 6213–6224.
- Wolf, D. 1994. Lamé’s problem of gravitational viscoelasticity: The isochemical, incompressible planet. *Geophys. J. Int.* **116**, 321–348.